

A FAULT-RESILIENT IMPLEMENTATION OF THREE LEVEL NPC IGCT-BASED CONVERTERS

Anderson Vagner Rocha¹, Gleisson J. França², Manoel E. dos Santos⁴, Hélder de Paula³ and Braz J. Cardoso Filho³

¹Centro Federal de Educação Tecnológica de Minas Gerais – CEFET-MG
Av. Amazonas 5253 - Nova Suissa - Belo Horizonte – MG, Brazil. Zip 30421-169
andersonrocha@des.cefetmg.br

²Postgraduate Program in Electrical Engineering - UFMG

³Dept. of Electrical Engineering – UFMG

Av. Antônio Carlos 6627- Pampulha - Belo Horizonte – MG, Brazil. Zip 31270-010

⁴Management of Engineering – GERDAU AÇOMINAS S/A

Rod. MG 443, km 07 S/N – Ouro Branco – MG, Brazil. Zip 36420-000

Abstract – This paper presents a strategy for protecting high power IGCT-based converters which are currently used in a wide range of drive applications. The protection of such converters against internal faults has been addressed in the technical literature, but the main focus has been on the solutions to disconnect the converter from the mains. In this paper, the short circuit current paths through the power devices are identified and studied from the perspective of keeping the overall repair cost after a fault to a minimum. It is shown that a preferred short-circuit current path that limits the thermal energy in all IGCTs to safe levels exists. Furthermore, it is demonstrated that it is possible to guarantee, through proper busbar geometry and/or device selection, that the short-circuit current stress can always be moved to the power diodes. Simulation results are presented to support all the discussions and conclusions, avoiding the costs and risks of tests on a medium voltage prototype.

Keywords - Active Rectifiers, Fault-Resilient, IGCT, NPC Converters, Protection, Reliability.

I. INTRODUCTION

High-power IGCT-based converters are currently used in a wide range of drive applications [1]. The solutions offered to the industry include active rectifier units and multi-motor drive possibilities [2], [3]. Since the reliability and continuity of service of these high power drives is an issue, efforts have been dedicated to the study and development of converter protection schemes ([4] - [9], [20]). Most of such effort has been dedicated to the proposition of suitable solutions to disconnect the damaged converter from the power mains ([4] - [7]). In [8] the authors address the current paths related to different possibilities of internal faults in the inverter and propose the addition of crow-bar circuits to limit the total converter damage extent.

The thyristor-type nature of the IGCT implies that short-circuit (fast rising) currents have to be limited by means other than the converter own switches [10]. In fact, short-

circuit protection is typically provided by turning on all IGCTs in the converter to limit the thermal stress on each device due to the energy in the dc bus capacitors and power mains, and by simultaneously triggering a fast circuit breaker or a device with the same function to disconnect the faulty converter from the power mains, limiting the total energy dissipated in it. Proper sizing of the power devices guarantees their integrity if the circuit breaker is operating properly. However, if the converter circuit breaker fails to operate as predicted in the design stage, the destruction of the power semiconductors is inevitable.

At this point, one can conclude that, besides proper sizing and maintenance of the converter circuit breaker, correct coordination of the power devices I^2t with the circuit breaker switching delay and short-circuit level at the converter connection point are the only issues to be addressed at the design stage. However, the existence of multiple short-circuit current paths in the converter [8] suggests that:

1. there might be a path that minimizes the overall devices replacement costs in case of a failure and
2. it might be possible to guarantee that the short-circuit currents will always flow through that particular path.

In this paper, the short-circuit behavior of IGCT-based three level NPC (Neutral Point Clamped) topologies is addressed from the perspective of characterization of the damage pattern following a shoot-through mode and a failure in the operation of the converter circuit breaker. Assuming that the initial failure caused the converter to enter the shoot-through mode, the possible current paths are identified and the progression of the damage to the power semiconductors is determined through computer simulations. The result of this study is pointing out a minimum repair cost shoot-through current path. The required design steps to guarantee that this preferred path will prevail are also outlined.

The block diagram of the circuit configuration of the IGCT based three-level NPC converter is shown in Figure 1. The power circuit consists of the next four parts:

- input transformer and reactor (IT)
- active rectifier unit (ARU)
- dc link capacitors (C1, C2)
- voltage source inverter (VSI)

Manuscript received 08/08/2010; revised 09/04/2011; accepted for publication on 16/05/2011 for the Special Section under recommendation of the editor in charge Antonio J. Marques Cardoso.

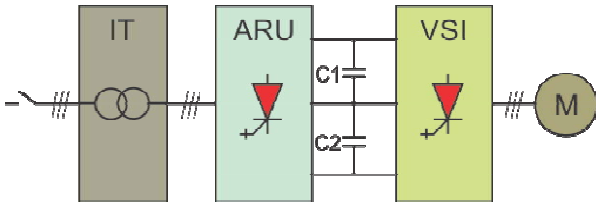


Fig. 1. Block-diagram of a typical IGCT-based NPC converter.

II. SHORT-CIRCUIT CURRENT PATHS IN NPC BRIDGES

In a short-circuit resulting from the converter entering the shoot-through mode (all IGCTs fired), two different current paths can be identified in Figure 2: one path goes through the freewheeling diodes (identified as FwxB and FwxC) and the top or bottom IGCTs, according to the instantaneous line voltage polarity (dotted and dashed paths); a second path goes through the clamping diodes (identified as CdxB and as CdxC) and the internal IGCTs (shaded paths).

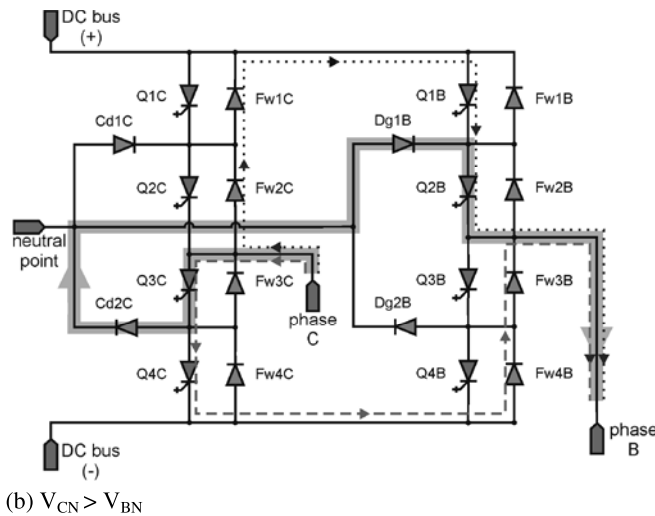
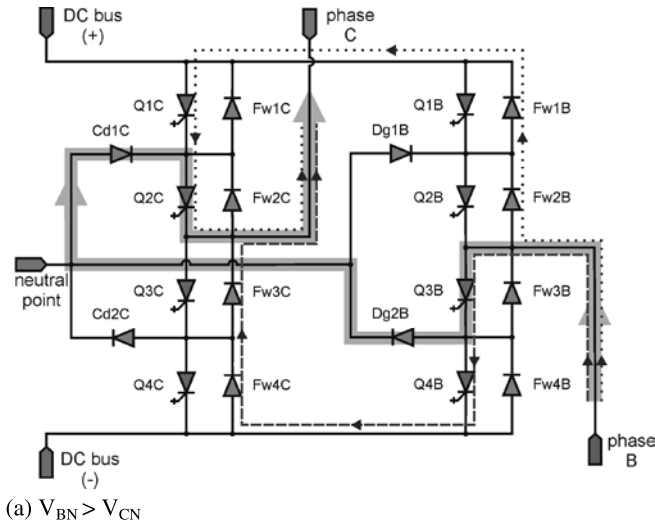


Fig. 2. NPC regenerative rectifier short-circuit paths during shoot-through mode (phases B and C). Similar paths can be identified when considering A-B and A-C phases combination.

Figure 2 illustrates the current flow through phases B and C only, for the sake of clarity. Similar figures can be obtained for any other pair of phases. Superposition can be used to obtain the three-phase short-circuit current distribution. From Figure 2, one can verify that in both cases the short-circuit currents flow through a series connection of two IGCTs and two freewheeling or clamping diodes. The short-circuit current distribution between these paths depends on the power devices conduction characteristics and on the existing impedances in the power connections, which can be added as discrete components or introduced by proper design of the busbars geometry and/or cable connections.

III. THE PROTECTION STRATEGY

The aim of the present paper is to propose a new method to reduce the overall repair cost associated to the converter initiation of the shoot-through mode followed by a circuit breaker malfunction. This situation would occur, for instance, as a result of a failure in one of the power semiconductors. Note that the IGCTs and diodes failure will result in the device short-circuiting due to the presspack packaging [10]. Open-circuited IGCTs would almost certainly indicate a faulted gate driver unit.

A real case recently experienced by the authors involving a failure in a similar converter leads to the following conclusion: taking into consideration that a permanent failure may result in a long production process interruption and, therefore, cause a loss of several million dollars, the reliability of the converter is in this case a mandatory issue.

The authors defend that in the situation at hand (fault \rightarrow shoot-through \rightarrow circuit breaker fails to open), the minimum cost-to-repair situation is the one that leads to no damaged IGCTs, being the lost power semiconductors all diodes. The reasons are:

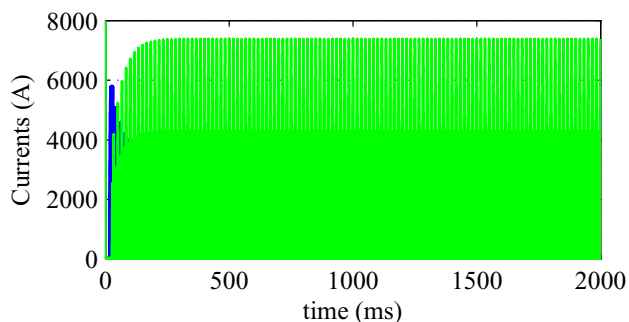
1. IGCTs are more expensive;
2. IGCTs require much more time to be replaced in case of none or minimum in-house stock due to cost issues.

Hence, if the converter enters the shoot-through mode, no matter the reason, and the circuit breaker fails to operate properly, it is desirable that no IGCTs be damaged.

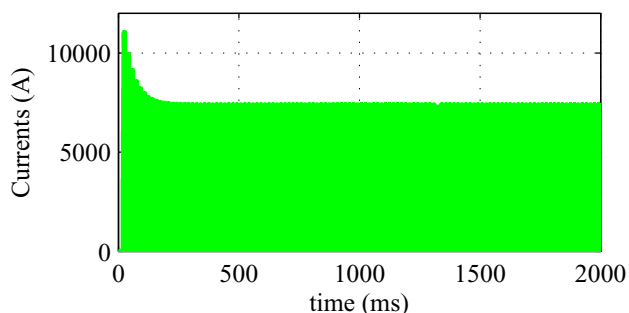
A. I^2t Ratings and Semiconductors Data

The power semiconductors data used in this work are shown in Table I. The phase C currents of top and bottom half devices and the computation of the consequences of keeping the converter in the shoot-through mode for 2 seconds¹, as a result of a failure in the circuit breaker, is shown in Figure 3. From this figure, it can be concluded that if the circuit breaker does not open as expected, the thermal energy in the semiconductors will reach extremely high levels, eventually exceeding their I^2t capability ($I^2t \geq 1.0$ p.u) and causing a permanent failure of the power converter.

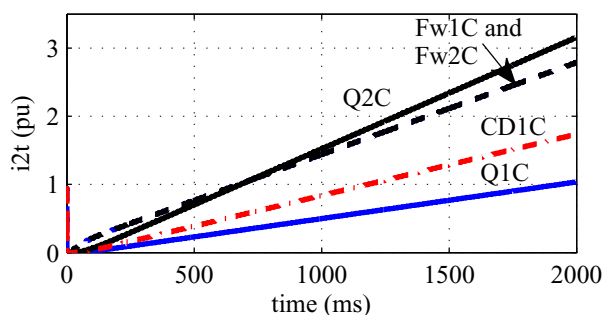
¹ According to international standards [12] the input transformer and reactor should be able to withstand short circuit currents for 2 seconds, at least.



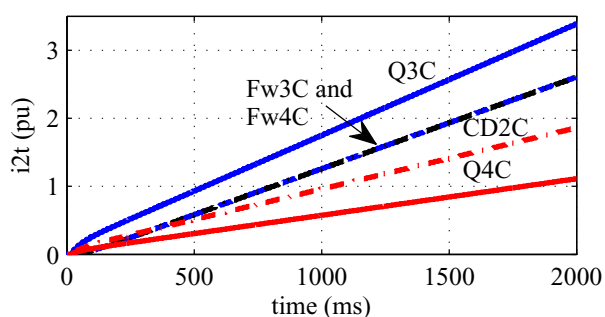
(a) Currents of the ARU top half devices - phase C



(b) Currents of the ARU bottom half devices - phase C



(c) $\int i^2 dt$ of the ARU top half devices - phase C



(d) $\int i^2 dt$ of the ARU bottom half devices - phase C

Fig. 3. NPC ARU phase C: currents and I^2t evolutions for the power devices under shoot-through (all diodes branches with the similar impedances).

In particular, it is shown in Figure 3 that it is possible that the first device to fail is one of the internal IGCTs. This situation is a consequence of the current path through the clamping diodes (shaded paths in Figure 2). Measures should

be taken to avoid this situation to occur; two alternatives are considered, as follows:

1. using clamping diodes with larger forward voltage drop than the one of the freewheeling diodes;
2. addition of a series impedance to the clamping diodes connections. The goal is to prevent the short-circuit current from flowing through the clamping diodes, thus avoiding prohibitive currents in the internal IGCTs.

TABLE I
Relevant power semiconductor data

Items	Forward Voltage [V]	Bulk Resistance [mΩ]	Reverse Resistance [kΩ]	I^2t [A ² .s]
QxB QxC	$V_q = 1.15$	$R_q = 0.21$	$R_{rq} = 100$	7.90×10^6
FwxB FwxC	$V_f = 1.4$	$R_f = 0.48$	$R_{rf} = 100$	2.65×10^6
CdxB CdxC	$V_c = 1.4$	$R_c = 0.48$	$R_{rc} = 100$	2.65×10^6

B. Converter Short-Circuit Current Distribution

The short-circuit current distribution within the ARU can be evaluated from the equivalent circuit shown in Figure 4. In this circuit, equivalent diodes (ED) were used to represent the different combination of power semiconductor in short-circuit current paths. Each equivalent diode represents:

- two freewheeling diodes and one IGCT (EDQF);
- two clamping diodes (EDC);
- one IGCT (EDQ).

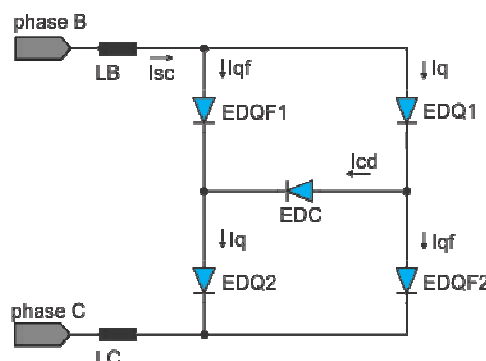


Fig. 4. Equivalent model for the short-circuit paths from Fig. 2 (a).

Taking into consideration that each power semiconductor device in the short circuit path can be represented, for the purposes of this study, by a voltage source and a bulk resistance, the equivalent diodes in Figure 4 will have the correspondent parameters shown in Table II.

TABLE II
Equivalent diodes parameters for Fig. 4

Equivalent Diode	Referred Components on Conduction	Forward Voltage [V]	Bulk Resistance [mΩ]
EDQFx	2 freewheeling diodes and 1 IGCT	$V_{qf} = 3.95$	$R_{qf} = 1.17$
EDQx	1 internal IGCT	$V_q = 1.15$	$R_q = 0.21$
EDC	2 clamping diodes	$V_c = 2.8$	$R_c = 0.96$

Based on the data of Table II and on the model illustrated in Figure 4, it is possible to obtain the relative distributions of the short-circuit current components in the different semiconductor devices of the ARU.

As shown in [9], the most important relationships between the currents in Figure 4 are:

$$\frac{I_q}{I_{qf}} = \frac{R_{qf} + R_c}{R_{qf}} = \rho \quad (1)$$

$$I_{qf} = I_{sc} \cdot \left(\frac{1}{1 + \rho} \right) \quad (2)$$

$$I_q = I_{sc} \cdot \left(\frac{\rho}{1 + \rho} \right) \quad (3)$$

$$I_{cd} = I_q \cdot \left(\frac{\rho - 1}{\rho} \right) = \alpha \cdot I_q \quad (4)$$

In the expressions above, ρ is the unbalance proportion factor regarding I_q and I_{qf} and α means the same between I_{cd} and I_q . Note that if there is any current flowing through EDC branch in Figure 4, then $I_q > I_{qf}$.

According to Tables I and II and (1) to (4), if all diodes in the ARU have the same characteristics, then $\rho=1.8205$, $I_q=0.6455I_{sc}$ and $I_{qf}=0.3545I_{sc}$. For this same case, the α coefficient between I_{cd} and I_q is:

$$\alpha = \frac{I_{cd}}{I_q} = 0.4508 \quad (5)$$

Thus, if there are no differences between the freewheeling and clamping diodes characteristics in this converter, the short-circuit current in the clamping diodes is 45.08% of the internal IGCTs currents and 29.1% of the total short-circuit current.

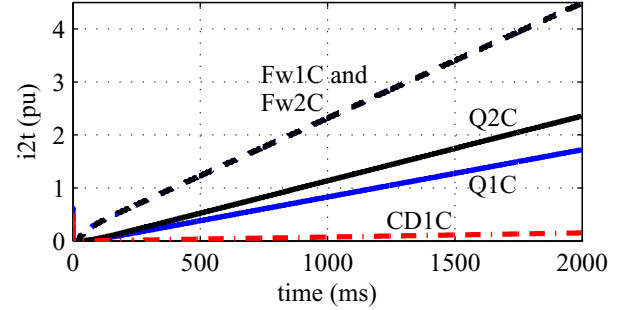
C. Changing the Short-Circuit Current Distribution

If the converter is on shoot-through mode, the short-circuit current component through IGCTs can be reduced by increasing the voltage drop in the clamping diodes branches, in order to ensure that the first converter devices to reach their thermal energy limits will always be the freewheeling diodes. The relationship between α and ρ shown in (4) can be used to determine new values for overall clamping diodes branch resistance (R_c) in order to meet a specific criterion of short-circuit current distribution.

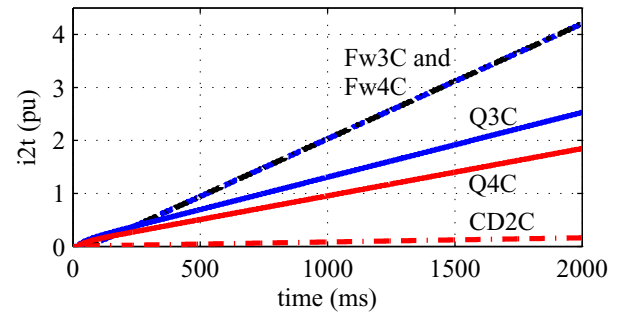
In the circuit of Figure 4, the proportion between I_q and I_{qf} components of I_{sc} current can be redefined in a more balanced way by using new values for α and ρ . The R_c value in this case is determined by:

$$R_c = \frac{1}{2} \left[\left(\frac{R_{qf} - R_q}{\alpha} \right) - R_{qf} \right] \quad (6)$$

Assuming that $I_q=0.55I_{sc}$ and $I_{qf}=0.45I_{sc}$, the short-circuit current component in the clamping diode will reduce from 29.1% to 10%. In this case, $\rho=1.22$, $\alpha=0.18$ and $R_c=2.1m\Omega$. The results shown in Figure 3 (c) and (d) are presented in Figure 5 (a) and (b), now considering the new value for R_c .



(a) $\int i^2 dt$ of the ARU top half devices – phase C.



(b) $\int i^2 dt$ of the ARU bottom half devices – phase C.

Fig. 5. NPC ARU phase C: $\int i^2 dt$ evolutions for the power devices under shoot-through (clamping diodes branches with changed impedances).

IV. IGCT PROTECTION

A. A Suggested Structure for the Converter Clamp

The structure of the NPC converter consists of three 3-level converter phase legs, one of which is illustrated in Figure 6. Note the symmetry between the arrangements of the components in the upper and lower halves of the leg.

In a real converter, each phase leg is usually designed as a separate clamp assembly primarily due to standardization, reliability and power density issues. The perspective of an eventual replacement of any diode in the power converter in case of damage suggests an assembly of stacks using only discrete components instead of “reverse conducting” devices including IGCT with the anti-parallel diode integrated monolithically. Figure 7 illustrates a possibility of mounting for the top half leg of a converter phase; the bottom half is identical in both mechanical structure and position of the power semiconductors.

The complete converter phase leg is properly constructed from two half-legs, resulting in the structure shown in Figure 8. Although the complete assembly of a converter leg in a

single structure may be possible, it would result in a cell with ten devices. In long stacks with several devices and their heat sinks, it may be difficult to obtain good mechanical stability and fulfill the basic rules for the correct clamping of press-pack high power semiconductors [13].

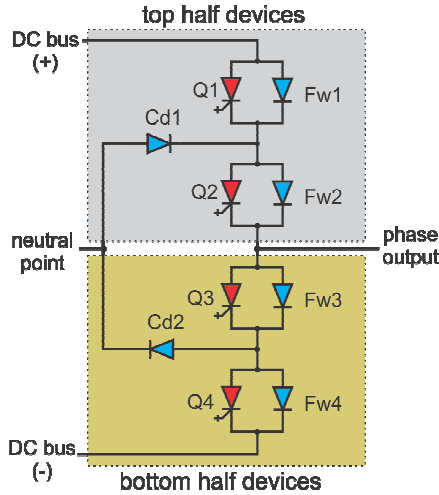


Fig. 6. Structure of a phase of the three-level NPC, IGCT-Based converter.

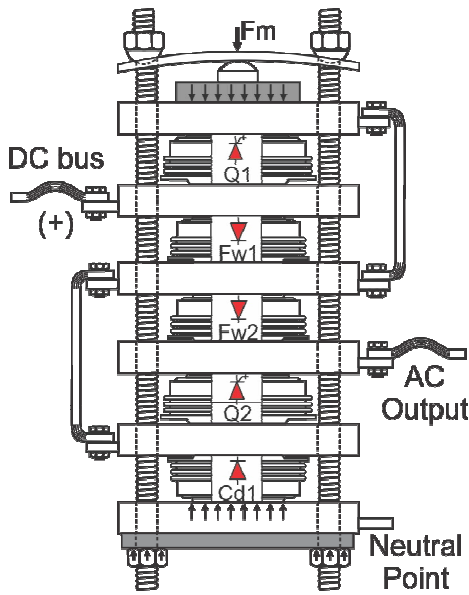


Fig. 7. Stack assembly: semi-leg using load spreaders and similar device diameters.

In the previous section, it was demonstrated that the new estimated value for the clamping diode series resistance (R_c) can be used to obtain the commercial devices with the most appropriate conduction characteristics. Nevertheless, the most convenient possibility for achieving the new R_c value (maintaining the original clamping diodes) is to alter the mechanical design and/or the conduction characteristics of the converter clamping diodes bars [9]. A simple alternative is to take advantage of the terminals available in the structure of the clamp. In the case of the structure suggested in Figure 8, the resistance of the clamping diode branch can be

conveniently inserted between the connection points **A** and **B** in the bottom bases of the stacks.

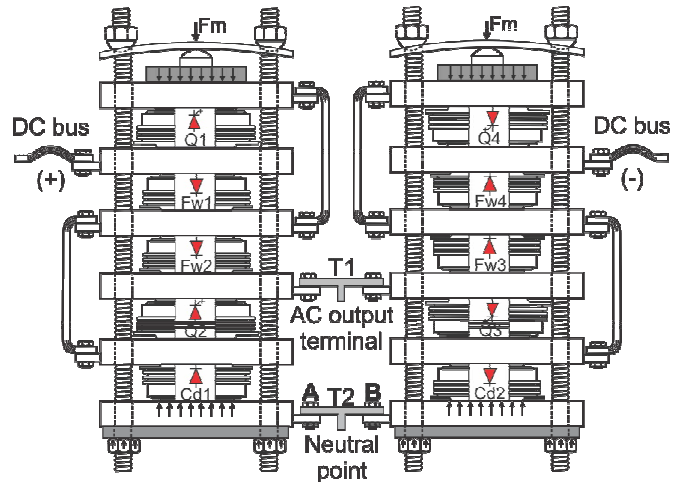


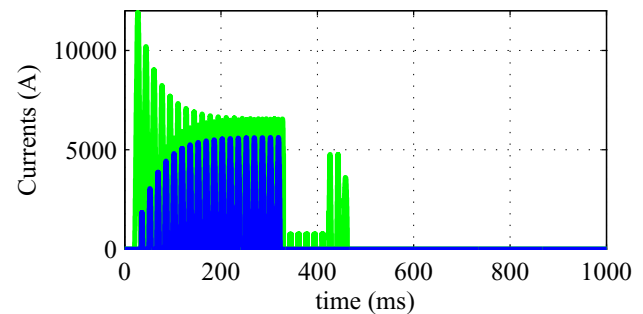
Fig. 8. Suggested leg assembly of the NPC three-level converter with discrete components.

B. Preserving the ARU IGCTs under Shoot-Through Mode

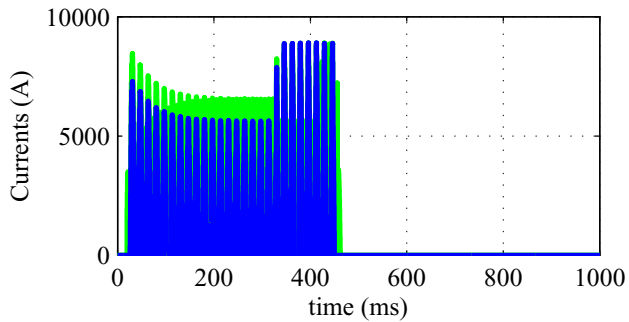
From the observation of Figure 5, a significant reduction of the rising rates of the thermal energy in the IGCTs during the short-circuit can be noticed due to the proper adjustment of the resistances in the clamping diodes branches. In fact, the shoot-through mode can occur for many different reasons in the ARU, like a mistaken command from the drive control unit, or a component failure within the inverter and/or on active rectifier.

Results corresponding to a failure (short-circuited device) of an internal freewheeling diode of the ARU (Fw1 in phase A) are shown in the sequence, assuming clamping diodes with increased resistance. Figures 9 and 10 show the current and the thermal energy increases in the IGCTs, respectively. It is shown that the thermal energy in the IGCTs is kept under its safe limits and also that it stabilizes in different time instants in phases A, B and C.

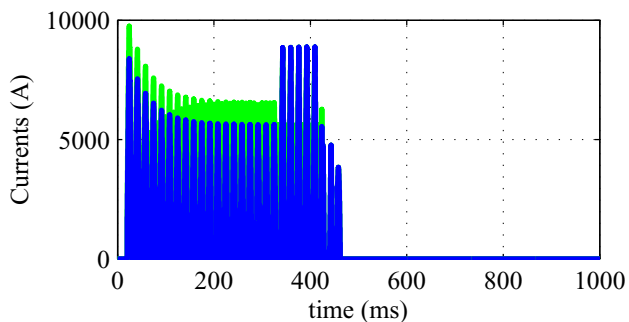
There is a point in each phase that the freewheeling diodes fails short-circuited sequentially, since the thermal energy exceeds their rated I^2t . As a result, the correspondent IGCTs stop carrying the short-circuit current and no more heat is generated in these devices, saving them from damages.



(a) Currents of the ARU IGCTs – Phase A

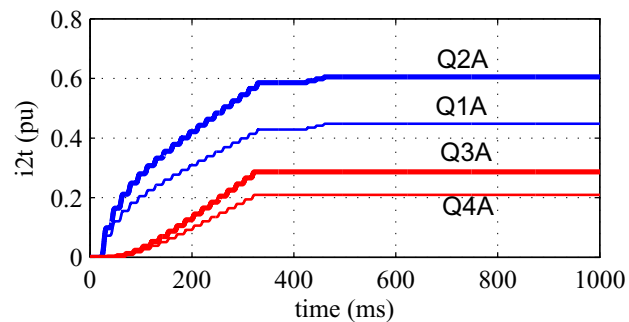


(b) Currents of the ARU IGCTs – Phase B

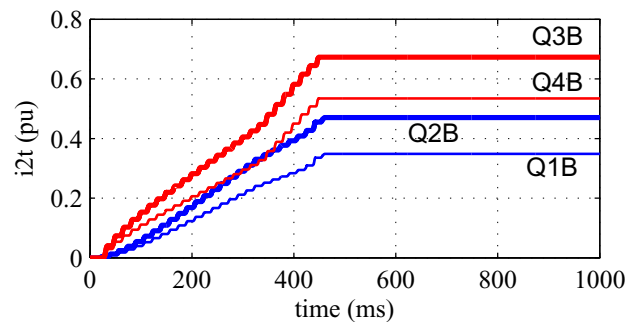


(c) Currents of the ARU IGCTs – Phase C

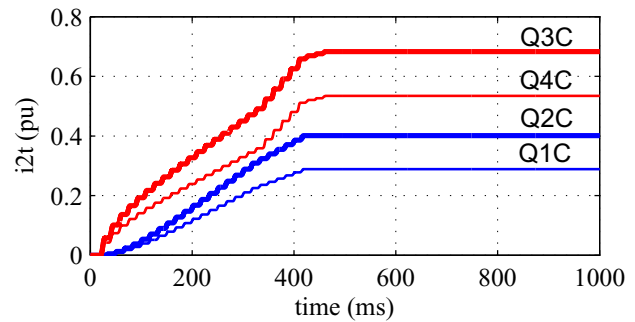
Fig. 9. NPC ARU IGCTs currents under internal short-circuit in a freewheeling diode and shoot-through.



(a) $\int i^2 dt$ of the ARU IGCTs – phase A



(b) $\int i^2 dt$ of the ARU IGCTs – phase B



(c) $\int i^2 dt$ of ARU IGCTs – phase C

Fig. 10. $\int i^2 dt$ of the ARU NPC IGCTs under internal short-circuit in a freewheeling diode and shoot-through.

V. IMPACT ON THE CONVERTER EFFICIENCY

In the previous sections, a method to guarantee the ARU IGCTs integrity, reducing the converter overall cost-to-repair after a failure followed by a circuit breaker malfunction was presented. The essence of the method consists in adjusting the conduction characteristics of the clamping diode branches (converter bars geometry and/or cable connections).

Although others aspects like the stray inductances arrangement and distribution may also be helpful to protect the IGCTs under short-circuit, it was verified that the increase of the resistances in the clamping diodes branches, in order to preserve the IGCTs, does not cause significant changes in the converter efficiency and in its thermal design.

Table III shows the losses and efficiency computation in a 3.3 MW, 2300 V / 60 Hz motor drive operating with SVPWM before and after the interventions proposed in the converter.

TABLE III
Losses computation for the converter

Clamping Diodes Branch Resistance (Ω)	Losses (W)			Converter Efficiency (%)
	Conduction	Commutation	Total	
0.00048	7220	16472	23692	99.29
0.00210	8202	16467	24669	99.26

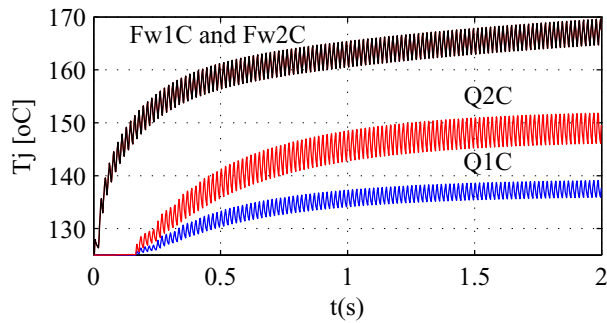
VI. DISCUSSIONS

Under transient conditions, the semiconductor junction temperatures are allowed to increase substantially above the 125 °C operating limit, reaching, in some cases, between 350 and 400 °C [19]. The manufacturers, however, do not provide the temperature limit of the junction, defining only the value of the transient current and the corresponding i^2t . Based on such information, it is not possible to state the precise instant of the ARU components failure under the imposed shoot-through. The proposed strategy for the implementation of the resilient converter is based on the imposition that, under a faulty situation, the freewheeling diodes fail before the IGCTs, inherently protecting the latter. The i^2t figure was employed in this work as a failure indicator of the devices because it represents the only information concerning the semiconductors thermal energy

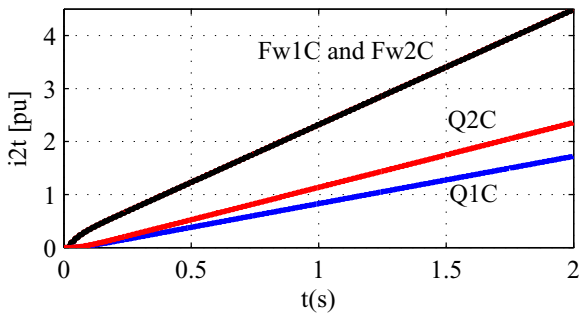
limits provided by the manufacturer. Even though the computation of the thermal integrals does not define the exact moment of the device failure, it provides a consistent indication of the sequence of failures of the converter semiconductors. Besides, the i^2t data does not depend on the component model parameters and thus can be more easily obtained.

Figure 11 shows the rates of the temperature rise in the junctions of the rectifier devices (phase C) under the same conditions of Figure 5, considering the transient thermal impedances of the employed commercial semiconductors. The correspondent i^2t rising rates are also showed in the same figure for the sake of comparison. It can be observed that the rate of the temperature rise in the junctions of the power diodes is higher than that of the IGCTs, indicating that the diodes are the first to fail, confirming the failure sequence defined by the thermal integrals (i^2t).

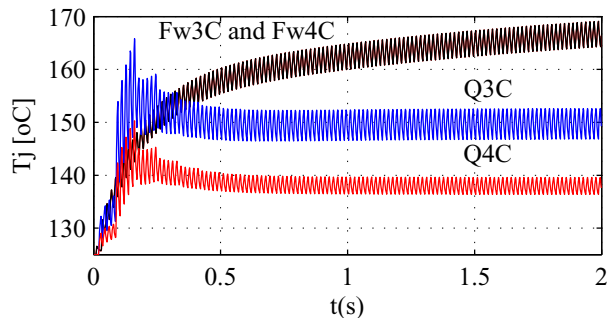
The typical curves of the thermal impedances available from the data sheet assume squared power pulses; since the actual current waveform differs from this pattern, it needed to be appropriately manipulated for its correct use. The junction temperature of the ARU components before the fault occurrence was assumed to be 125 °C.



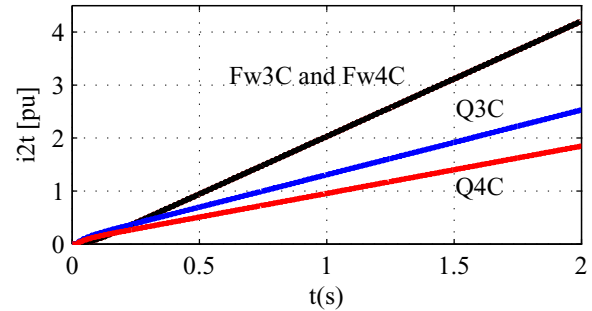
(a) Phase C – top half devices junction temperature



(b) Phase C – top half devices i^2t



(c) Phase C – bottom half devices junction temperature



(d) Phase C – bottom half devices i^2t

Fig. 11. Junction temperature and i^2t rising rates during a commanded shoot through in the ARU.

VII. CONCLUSIONS

In this paper, the short-circuit behavior of IGCT-based three-level NPC topologies is addressed from the perspective of the damage pattern characterization associated to a shoot-through mode and a following failure in the operation of the converter circuit breaker. In order to keep the cost-to-repair at its minimum under these conditions, it is mandatory to limit the damage of the power semiconductors to the power diodes. The measures proposed here permit the converter to behave in a more resilient manner, reducing the costs and time interruption associated to the maintenance.

In this study, the possible shoot-through current paths were identified and the progression of the damage to the power semiconductors was determined through computer simulations. The short-circuit current paths that leads to the destruction of the IGCTs were identified, being the necessary measures to avoid such paths pointed out.

An active rectifier unit – ARU – was considered in this study without loss of generality. The results can be promptly applied to inverter units – INU, although the considered situation primarily threatens the ARUs power semiconductors.

It was demonstrated that, by proper design of the geometry of busbars and/or selection of the appropriate freewheeling and clamping diodes, it is possible for the IGCTs to survive the converter shoot-through mode even in the event in which the circuit breaker fails to operate, thus reducing the total repair cost. Important insights may have been given to the electrical engineers and mechanical designers on how to construct an NPC IGCT-based converter and to arrange the clamping diodes and internal IGCTs bars advantageously.

As a final comment, it was observed that the investigation concerning the transient junction temperature rises confirmed the devices failure sequence previously defined by the i^2t analysis.

APPENDIX

Power Semiconductors Considered:

IGCTs Model: 5SHY 35L4512

Limiting load integral: $7.9 \times 10^6 \text{ A}^2\text{s}$

Max. peak surge on-state current: 35×10^3 A
Max. average on-state current: 2100 A
Max. repetitive peak off-state voltage: 4500 V
Forward resistance @ $T_j=125^\circ\text{C}$: $0.21\text{m}\Omega$
Threshold voltage @ $T_j=125^\circ\text{C}$: 1.15 V

Diodes Model: D 921 S 45 T

Limiting load integral: 2.65×10^6 A²s
Max peak surge on-state current: 23×10^3 A
Max. average on-state current: 1380 A
Max. repetitive peak reverse voltage: 4500 V
Forward resistance @ $T_j=140^\circ\text{C}$: $0.48\text{m}\Omega$
Threshold voltage @ $T_j=125^\circ\text{C}$: 1.40 V

ACKNOWLEDGMENT

The authors would like to thank CEFET-MG and UFMG for the financial support.

REFERENCES

- [1] Y. S. Suh, J. Steinke, and P. Steimer, "Efficiency comparison of voltage source and current source drive system for medium voltage applications," *IEEE Transactions on Industrial Electronics*, vol. 54, no. 5, pp. 2521–2531, Oct. 2007.
- [2] R. D. Klug and A. Mertens, "Reliability of megawatt drive concepts," in *IEEE International Conference on Industrial Technology*, pp. 636-641, 2003.
- [3] Markus Ahrens and Scott Southby "Cutting edge, energy efficient conveyor systems", ABB Australia - Apr 27, 2010.
- [4] Z. Hu, C. Mao, J. Lu and S. Fan, "Fuse protection of IGCTs against rupture in three-level commutated inverter," *Proceedings of the PowerCon 2002*, vol. 1, no. 23, pp. 611–615, October 2002.
- [5] P. K. Steimer, J. K. Steinke and H. E. Gruning, "A reliable, interface-friendly medium voltage drive based the robust IGCT and DTC technologies," in *34th IEEE IAS Annual Meeting*, pp. 1505-1512, 1999.
- [6] A. U. S. L. C. ATPS, ACS 6000 medium voltage drive - course G750: operation and maintenance, ABB, Turgi/Switzerland.
- [7] M. Santos and B. J. Cardoso Filho, "Short-circuit and overcurrent protection of IGCT-based three-level NPC inverter," in *35th annual IEEE Power Electronics Specialists Conference*, pp. 2553-2558, 2004.
- [8] P. Bordignon, M. Carpaneto, M. Marchesoni and P. Tenca, "Faults analysis and remedial strategies in high power neutral point clamped converters," in *IEEE Power Electronics Specialists Conference*, pp. 2278-2783, 2008.
- [9] A. V. Rocha, G. J. França, M. Santos, H. de Paula and B. J. Cardoso Filho, "Improving the Performance of Protection Schemes in Three Level IGCT-based Neutral Point Clamped Converters," *Proceedings IEEE Energy Conversion Congress and Exposition (ECCE 2010)*, 12-16 September 2010, Atlanta, GA.
- [10] P. K. Steimer, H. E. Gruening, J. Werninger, E. Carroll, S. Klaka, and S. Linder, "IGCT-a new emerging technology for high power, low cost inverters," *IEEE Ind. Appl. Mag.*, vol. 5, no. 4, pp. 12–18, Jul./Aug. 1999.
- [11] Y. Suh, P. Steimer, et al, "Application of IGCT in high power rectifiers," *IEEE Transactions on Industry Applications*, vol. 45, no. 5, pp. 1628-1636, Sept. 2009.
- [12] IEC 60076-5 Power transformers – part 5: Ability to withstand short circuit, ed. 3.0, 2006.
- [13] B. Backlund and T. Schweizer, "Recommendations regarding mechanical clamping of Press Pack High Power Semiconductors," ABB Application Note, No. 5SYA2036-01, Nov. 2002.
- [14] Shutian Zhang, Qiongquan Ge, Yaohua Li, "Three-level NPC Inverter with IGCT for High Power AC Drives," *The 11th International Conference on Electrical Machines and Systems (ICEMS2008)*, Oct. 17-20, 2008.
- [15] J. Rodriguez, S. Bernet, B. Wu, J. O. Pontt and S. Kouro, "Multilevel Voltage Source Converter Topologies for Industrial Medium-Voltage Drives," *IEEE Trans. Ind. Electron.*, vol. 54, no. 6, pp. 2930–2945, Dec. 2007.
- [16] L. G. Franquelo, J. Rodriguez, J. I. Leon, S. Kouro, R. Portillo and M. M. Prats, "The age of multilevel converters arrives," *IEEE Trans. Ind. Electron. Magazine*, vol. 2, no. 2, pp. 28–39, June 2008.
- [17] ABB, "New inverter modules for optimum performance," [Online]. Available: www.abb.com.
- [18] Tschirley, S.; Bernet, S.; Streit, P.: "Design and characteristics of reverse conducting 10-kV-IGCTs", *Proc. of IEEE Power Electronics Specialists Conference, PESC 2008*, Rhodos, Griechenland, 15.-19. Juni 2008, S. 92-97
- [19] P. Wood, *Fundamentals and Applications of Gate-Turn-off Thyristors*. Palo Alto, CA: EPRI, EM-5317, 1988.
- [20] M. E. Santos, *Análise e Projeto de Um Inversor Trifásico para Aplicações em Médias Tensões Industriais*, Tese de doutorado, PPGEE, UFMG, 2004.

BIOGRAPHIES

Anderson Vagner Rocha was born in Belo Horizonte, Brazil, on February 13th, 1970. He received the Electrical Engineer degree (1994) and the Master's (1997) degrees in Electrical Engineering from Federal University of Minas Gerais, Belo Horizonte, MG, Brazil. He is currently working towards his doctorate in Power Electronics at this same University.

He is faculty member of the Federal Technological Center of Minas Gerais, Brazil, where he teaches Electrical Machines and Drives. His current research interests include efficiency, reliability and availability of medium-voltage power converters and its applications.

Braz de Jesus Cardoso Filho was born in Fortaleza, Brazil, in 1965. He received the Electrical Engineer degree and the Master in Electrical Engineering degree from the Universidade Federal de Minas Gerais, Belo Horizonte, Brazil, in 1987 and 1991, respectively, and the Ph.D. degree from the University of Wisconsin, Madison, in 1998.

Since 1989, he has held a faculty position in the Department of Electrical Engineering, Universidade Federal de Minas Gerais, where he was the founder of the Industry

Applications Laboratory. He has authored or coauthored more than 90 technical papers on the topics of power electronics and electrical drives. His current research and technical interests are in utility applications of power electronics, high-power converters and drives, and semiconductor power devices.

Helder de Paula was born in Uberlândia, Brazil, on December 27, 1975. He received his Electrical Engineer degree (1998), Master (2001) and Doctor (2005) in Electrical Engineering degrees all from Universidade Federal de Uberlândia, Brazil.

In 2006, he joined the Electrical Engineering Department of Universidade Federal de Minas Gerais (UFMG), as a Professor and member of the Industry Applications Laboratory. He has worked in R&D projects on equipment modeling for high frequency studies. His main interests are motor drives, electromagnetic compatibility and power quality.

Manoel Eustáquio dos Santos was born in Pompéu, state of Minas Gerais, Brasil, on September 27th, 1953. He received the Electrical Engineer degree from the Pontifícia Universidade Católica de Minas Gerais, Brasil, in 1978 and the Master of Science and Doctor in Electrical Engineering degrees from the Universidade Federal de Minas Gerais, Brasil, in 1990 and 2005, respectively.

Since 1981 he works as technical Consultant at Gerdau-Açominas, an integrated Steel Mill in Ouro Branco, MG, Brasil. His current research and technical interests are in electrical power systems, utility applications of power electronics, high power converters and drives and semiconductor power devices.

Gleisson Jardim França received the Electrical Engineer (2002) and Master in Electrical Engineering degree (2004) from Universidade Federal de Minas Gerais.

He has professional experience in design and development of frequency converters for medium voltage and teaching in higher education, working in the areas of electrical machines, electrical drives and power electronics. He is currently a doctoral student at Federal University of Minas Gerais, researching hybrid harmonic filters for power systems.